Al-Azhar University Civil Engineering Research Magazine (CERM)
Vol. (39) No. (1) January, 2017

Experimental and theoretical study on behavior of one-way composite pre-slabs using different shear connector shapes and interface position

Kamal G. Metwally[1]& Ahmed A. Afifi[2]

1- Ass. Professor, Civil Eng. Dept., Faculty of Eng., Beni-Suef University, Beni-Suef, Egypt.
2- Ass. Lecture, Structural Eng. Dept., Faculty of Eng., October 6 University, Giza, Egypt.

ملخص البحث

يحتوي هذا البحث على دراسة عملية ونظرية عن سلوك البلاطات بسيطة الارتكاز ذات الأتجاه الواحد باستخدام اشكال مختلفة من روابط القص واسطح التلامس تحت تأثير الأحمال الموزعة ،كما يتضمن هذا البحث البرنامج العملي و النظري الذي تم تنفيذه و يحتوي على سبعه بلاطات بأبعاد (٨٣٠×١٠٥٠) مم و (١٢٠) مم سمك تم اختبارهم حتى الانهيار.

ABSTRACT

This research work was conducted to study experimental and theoretical of the shear connector and interface position composite concrete pre-slab which are used extensively in the construction of both buildings and bridges. The problem of shear transfer is a major item in the study of the behavior of pre-slabs to achieve the composite action between two layers. The experimental program contains testing of six Pre-Slabs and one reference monolithic slab all specimens with overall dimensions of slabs 105cm x 83cm with thickness 12cm were simply supported and tested under the effect of uniform distributed load. The studied pre-slabs composed of two layers cast at different ages with variable thickness using different shape of shear connectors. Finally, the slabs are modeled with the finite element computer program.

KEYWORDS: pre-slab, composite, Shear connector, interface.

5. INTRODUCTION

Concrete-concrete composite flexural members are widely used in the building and bridge construction as well as strengthening. The common types of the composite concrete-concrete sections are composite slabs with deck floor and composite slab with prefabricated beams.

To achieve the composite action between old and new part, different types of shear connection between the two concrete surfaces may be used, such as rough surface connection, shear keyed connection, steel doweled shear connection and using of Epoxy binding materials.

6. Experimental Program

The performed experimental work consisted of seven medium scale reinforced concrete slabs All specimens with overall dimensions of slabs (105cm X 83cm) and (12cm) thickness were supported on two edge supports to represent the case of one way simply supported and tested under the effect of uniformly distributed loads in two groups over and above one monolithic specimens. The main two variables are the Interface position and shapes of shear connectors. The pre-slabs represent one monolithic specimen M1 and two groups G1and G2. Table (1) lists the details of the specimens. In addition figures (1) through fig (9), present the

overall dimension and reinforcement details of the tested beams.

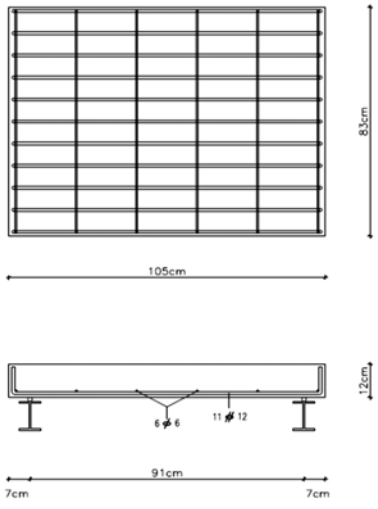

Figure 1: Typical dimensions and reinforcement of monolithic slab (M1)

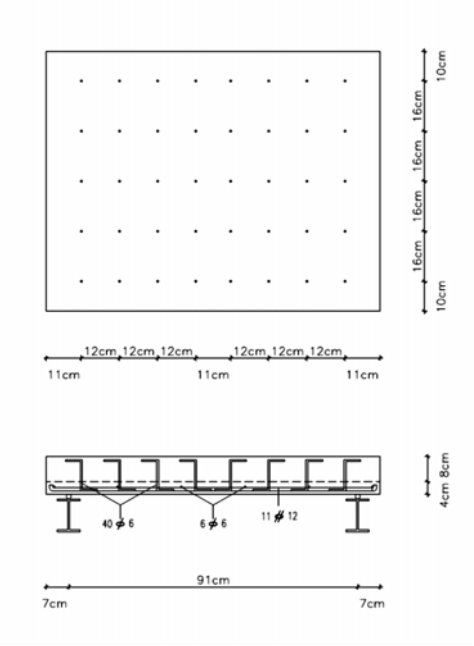

Figure 2: Typical dimensions and reinforcement of composite pre-slab (S11)

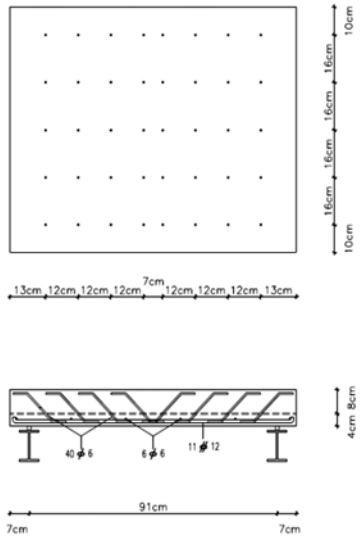

Figure 3: Typical dimensions and reinforcement of composite pre-slab (S12)

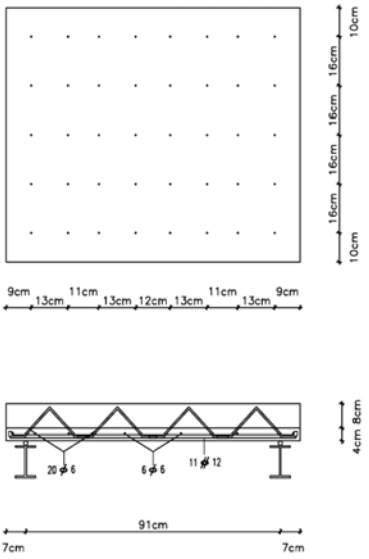

Figure 4: Typical dimensions and reinforcement of composite pre-slabs (S13)

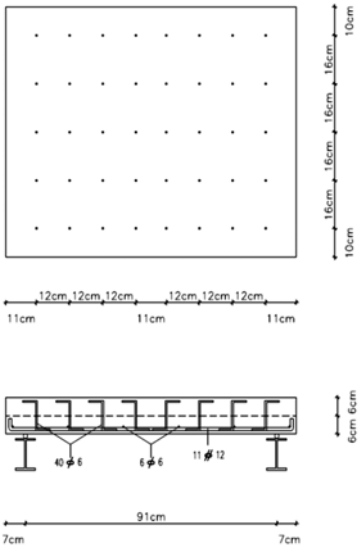

Figure 5: Typical dimensions and reinforcement of composite pre-slab (S21)

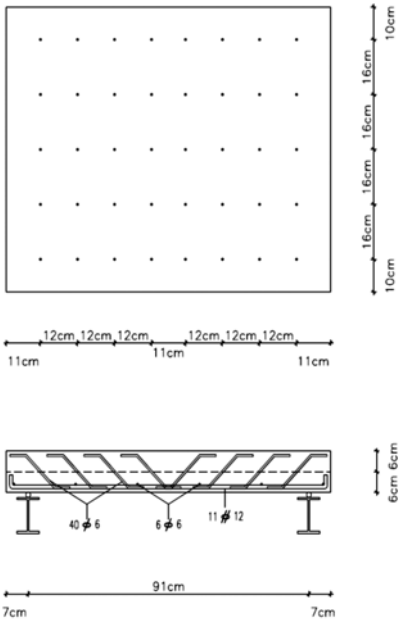

Figure 6: Typical dimensions and reinforcement of composite pre-slab (S22)

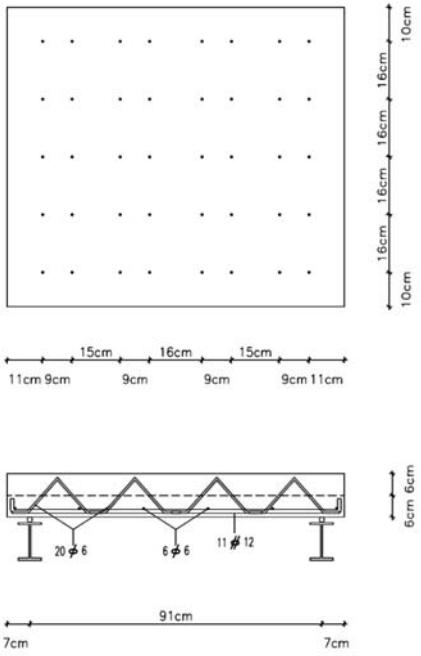

Figure 7: Typical dimensions and reinforcement of composite pre-slab (S23)

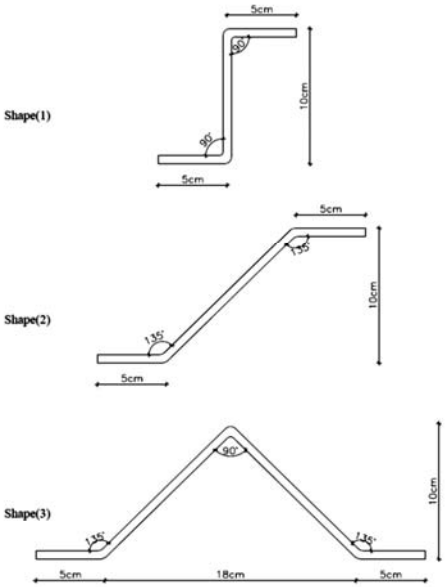

Figure 8: Typical dimensions of shear connector shaped

Table (1): Designation of experimental testing groups

Specimen		F_{cu}(first layer) kg/cm^2	F_{cu} (second layer) kg/cm^2	t_b(cm)	t_t(cm)	Shear connector shape
Monolithic	M1	380		12		----
Group 1	s11	380	380	4	8	1
	s12	380	380	4	8	2
	s13	380	380	4	8	3
Group 2	s21	380	380	6	6	1
	s22	380	380	6	6	2
	s23	380	380	6	6	3

7. Experimental Details

3.1 Mix Composition

Many trial mixes were done to have various values of f_{cu} with changing the percentage of W/C (water cement ratio) and amount of silica fume and the final quantities required by weight for one cubic meter of fresh concrete for the specimens are as given in table (2)

Table (2): Material quantities in kg/m3 for the cube strength specimens

Materials Quantity (Kg.)	Fcu Kg/cm2	Cement	Sand	Crushed lime stone	Water	Super-plasticizer	Silica fume
	380	400	600	1110	200	----	---
	600	500	600	1150	190	10.5	50

3.2 Preparation of Specimens

Wooden forms were designed and prepared to allow for simple and correct placing of concrete. The steel bars were tied with the stirrups forming reinforcement cages. Electrical strain gauges of 6 mms length and 120.3± 0.5 ohm resistance were fixed on the steel bars to follow the reinforcement strains during loading.

3.3 Mixing and Curing

Dry materials and water were mechanically mixed in a drum mixer for two minutes and cast in the forms just after mixing. The cast concrete was then vibrated with an electrical needle vibrator and hence the final concrete surface was smoothed. The specimens were moisture continuously with water for 7 days and kept in laboratory atmosphere for about 4 to 6 weeks until they were tested. Quality control specimens were prepared during casting specimens to obtain the mechanical properties of the used concrete. These specimens consisted of six cubes specimen (15.8 cm. side) and 2 cylindrical specimens (15 cm diameter and 30 cm height).Three cubes were tested in compression to get the 7 days compressive strength while another three cubes were tested to get the 28 days compressive strength.All cylindrical specimens were tested after 28 days from casting. Table (3) shows the average the values of the obtained results.

Table (3): Mechanical properties of L.W.C mix (kg/cm^2)

Concrete strength (Kg/Cm2)	Cube strength	
	7 days	28 days
380	286	382
600	433	596

3.4 Loading of specimens

One side of each specimen is white painted, one day before testing, to facilitate the tracing of cracks during loading. The specimens were loaded in increments up to failure. The tested specimens were instrumented to measure their deformational behavior after each load increment. The recorded measurements include concrete, longitudinal reinforcement and

transverse reinforcement strain, deflection and crack propagation. The concrete strains were measured using demec points mounted on the painted sides of the specimen. The reinforcement strains were measured using the electrical strain gauge fixed on it. The deflections were measured using 4 Linear Voltage Displacement Transducers (LVDT) 100 mm capacity and 0.01 mm accuracy and arranged to measure the deflection distribution to the specimen. After each load increment the cracks were traced and marked on the painted sides of the specimen according to their priority of occurrence.

3.5 Test procedure

The specimens were tested by using a hydraulic jack. At the beginning of each test, the specimen was installed on the two supports as a simple beam. Then, the jacks loading systems were then positioned as shown in figure (9). The dial gauges were adjusted in position. The strain gauges and load cell were hooked up to the data acquisition system. The reading of the hydraulic jacks and the steel strain gauges were taken by special instruments.

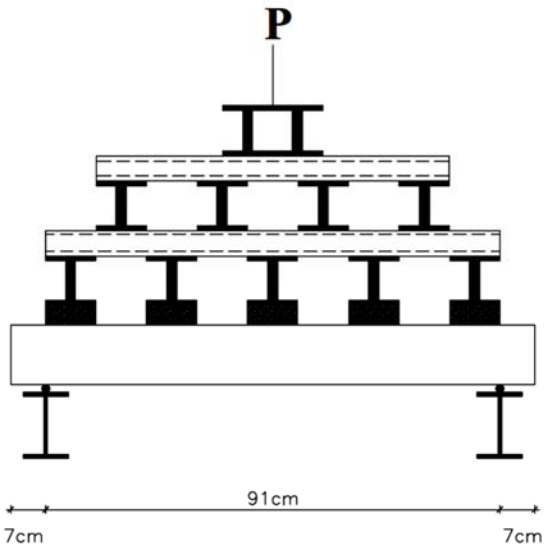

Figure 9: Test setup

8. Experimental Results

The fourteen tested models behaved in a different manner and the following remarks were noticed:

4.1 Cracking and Failure Loads

- Increasing in the bottom slab thickness led to an increasing in the failure loads as seen between G1 and G2 with ratios (37%, 25% and 22%).

- Effective of the shear connector shape has approximately the same effective of the bottom slab thickness.

After the peak of each loading, the crack pattern was marked to provide necessary information required for defining the failure mechanism of each specimen.

For specimen M1 the first crack was observed at load of 12.3 ton on the bottom surface at section of maximum moment i.e. nearly to the middle of the span. After this load level, another bottom cracks appeared as the increasing of load.

From figure (11) it can be noticed that the bottom cracks were symmetrically about the axe passing through the mid span of the slab. The diagonal shear crack started to appear at load of 25.0 ton it was near the support from the two sides as shown in figure (12).Increasing the load after the diagonal shear crack appeared led to increase in the diagonal shear crack width and initiation of new shear cracks between the two main diagonal shear cracks till the specimen had a complete shear failure in left side.

From figures (13) and (14) it can be noticed that the first crack was observed at load of 14.0 ton on the bottom surface at section of maximum moment and the diagonal shear crack started to appear at load of 25.0 ton it was near to the supports.

For specimen S11 the slab experienced the formation of fine cracks in the middle of slab span at load of 13.0 ton and then fine cracks diagonally started in the both shear zones left and right sides at load of 20.0 ton as shower of that specimen was characterized by shear failure in the left side with extension of the cracks in the slab as shown in figures (15) and (16).

For specimen S12 at load of 15.0 the slab experienced the formation of fine cracks in the middle of slab span and then at load of 40.0 fine cracks diagonally started in the both shear zones left and right sides of the slab and then the cracks continues in the bottom of the slab as shown in Fig (17), (18). The final failure of that specimen was characterized by shear failure in the right side with extension of the cracks in the slab.

For specimen S13 as shown in Fig (19), (20) the specimen followed the same behavior of the previous specimen with the different in the load failure and crack size, first crack at load of 18.5 ton.

For specimen S21 the slab experienced the formation of fine cracks in the middle of slab span at load of 20.0 ton and then fine cracks diagonally started in the both shear zones left and right sides at load of 45.0 ton as shower of that specimen was characterized by shear failure with extension of the cracks in the slab as shown in figures (21) and (22).

For specimen S22 at load of 25.0 the slab experienced the formation of fine cracks in the middle of slab span and then at load of 40.0 fine cracks diagonally started in the both shear zones left and right sides of the slab and then the cracks continues in the bottom of the slab as shown in Fig (23), (24). The final failure of that specimen was characterized by shear failure in the left side with extension of the cracks in the slab.

For specimen S23 as shown in Fig (25), (26) the specimen followed the same behavior of the previous specimen with the different in the load failure and crack size, first crack at load of 17.2 ton and the final failure in the left side.

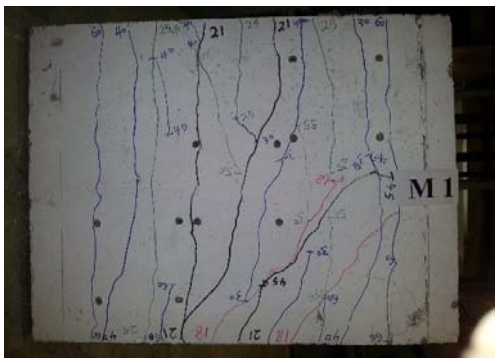

Figure 10: Cracks pattern of specimen M1

Figure 11: Shear cracks of specimen M1

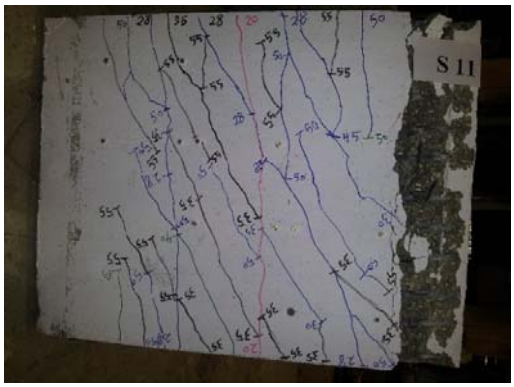

Figure 12: Cracks pattern of specimen S11

Figure 13: Shear cracks of specimen S11

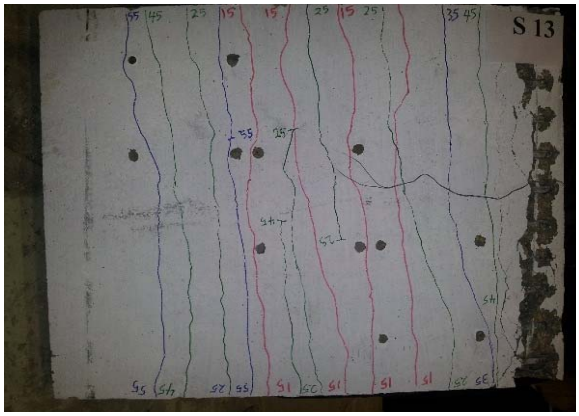

Figure 14: Cracks pattern of specimen S12

Figure 15: Shear cracks of specimen S12

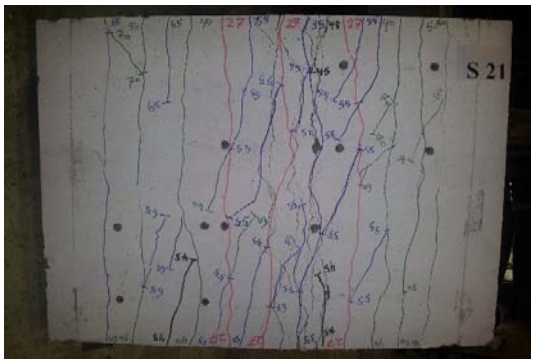

Figure 16: Cracks pattern of specimen S21

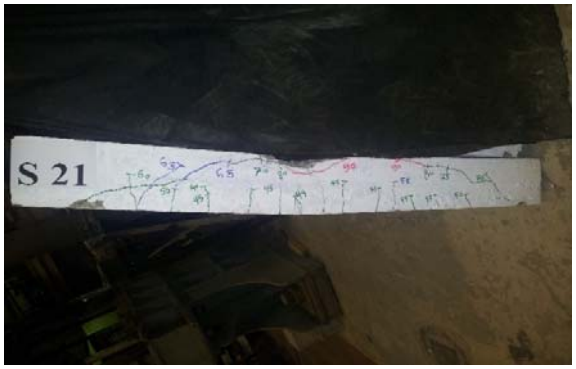

Figure 17: Shear cracks of specimen S12

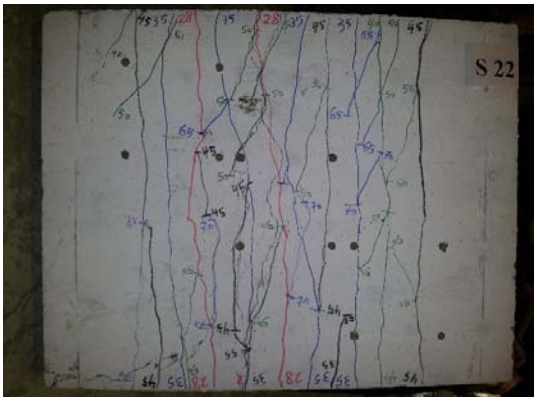

Figure 18: Cracks pattern of specimen S22

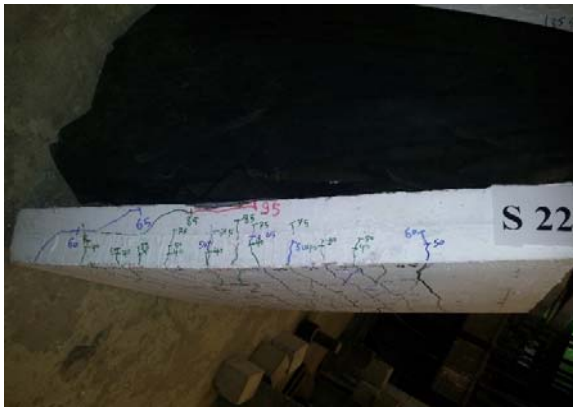

Figure 19: Shear cracks of specimen S22

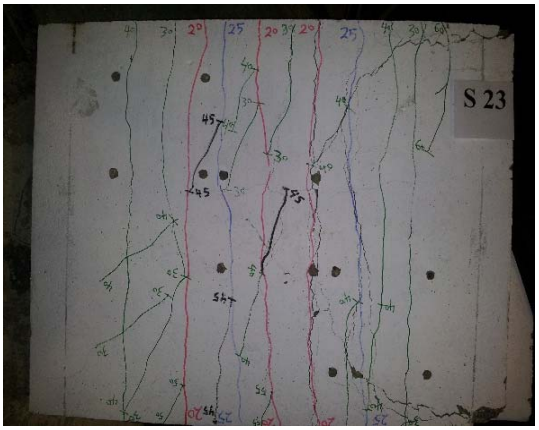

Figure 20: Cracks pattern of specimen S23

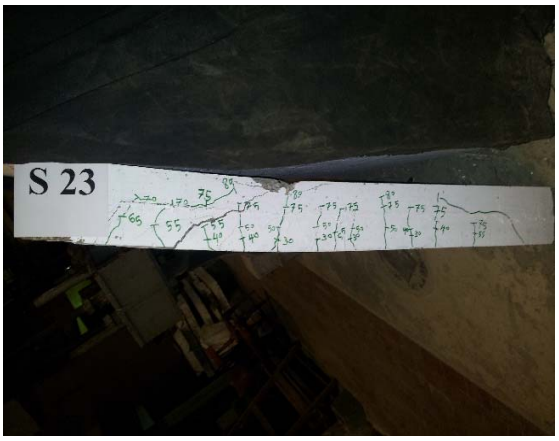

Figure 21: Shear cracks of specimen S23

4.2Deflections

As mentioned before, the vertical deformations were measured through three points of each slabs to predict the deflection shape of the tested monolithic and pre-slabs at 0.25, 0.5 and 0.75 of span. The profiles of the tested slabs at different stages of loading cracking and ultimate loads. The experimental load-deflection curves at points of maximum deflection of the slabs also the values of cracking and ultimate loads of slab, we observed the following.

The load deflection curves for the tested slabs were nearly linear at the early stages of loading from zero up to the first cracking of the concrete The great decrease in stiffness due to excessive cracking had resulted in relatively great increase in the deflection values, Approaching the failure load, the deflection continued to increase even with the applied load being maintained constant.
Comparing the deflections of slabs, the deflections of specimens with the shear connector shape (3) have the least values in each group because the cracks decreasing along the total span. The deflection values of specimens with the shear connector shape (3) are the nearest values to the monolithic group. The slope of the load deflection curves is nearest at the early stages of loading in each group.

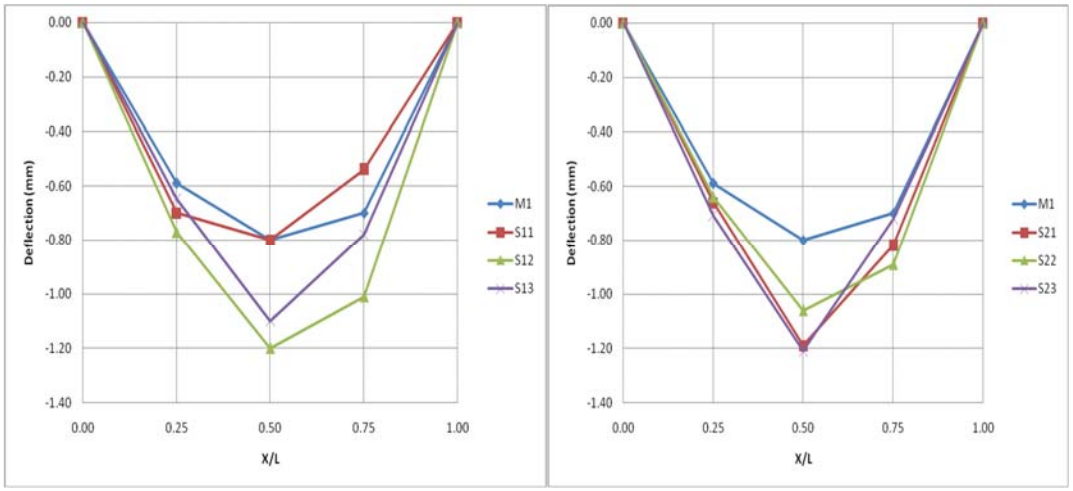

Figure 22: Deflection profile at cracking load of M1 and G1Figure 23: Deflection profile at cracking load of M2 and G3

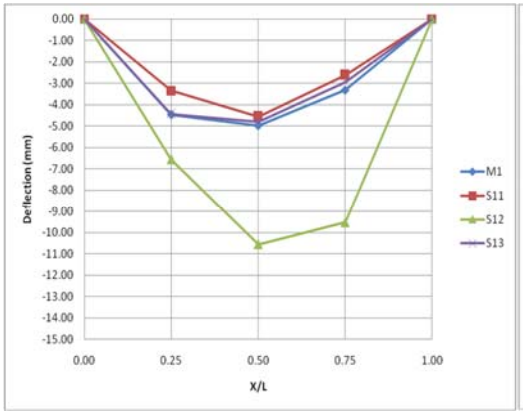

Figure 24: Deflection profile at cracking load of M1 and G1

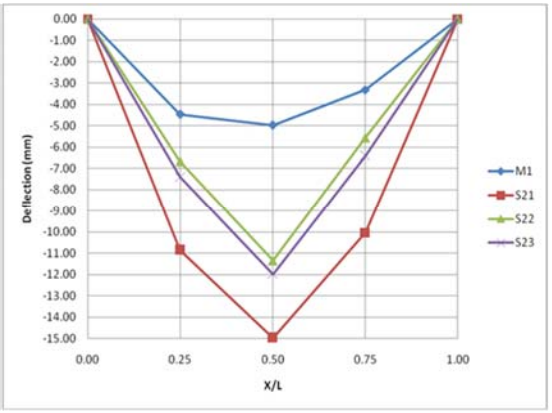

Figure 25: Deflection profile at cracking load of M1 and G2

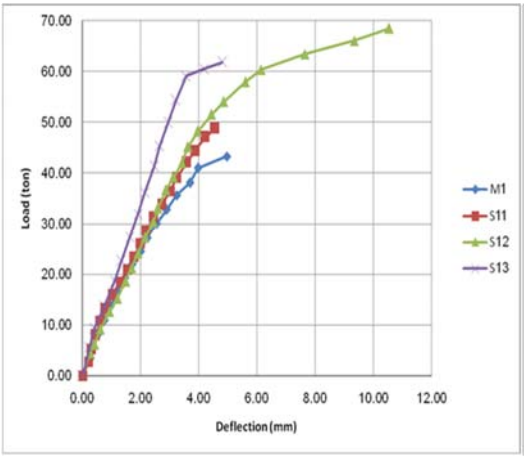

Figure 26: Load-Deflection curves at middle of M1 and G1

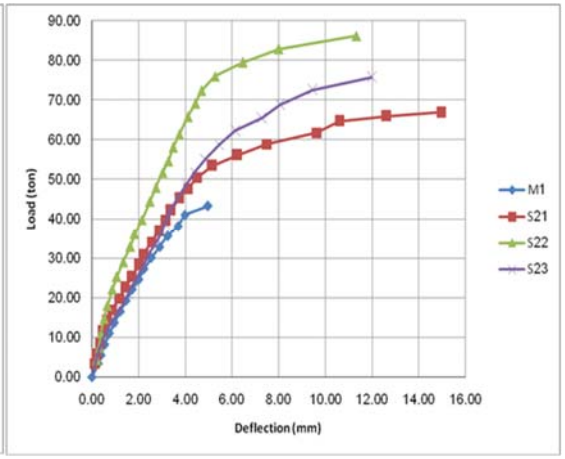

Figure 27: Load-Deflection curves at middle of M1 and G2

5-THEORETICAL PROGRAM

The literature review has provided useful insight for future application of a finite element package as a method of analysis. To ensure that the finite element model is producing results that can be used for study, any model should be calibrated with good experimental data. This will then provide the proper modeling parameters needed for later use.

It is decided to use ANSYS (16.0) as the F.E. modeling package.
In this chapter, it will be discussed:
The main steps for modeling a reinforced concrete slab using ANSYS (16.0).

5.1 Detailing of the model

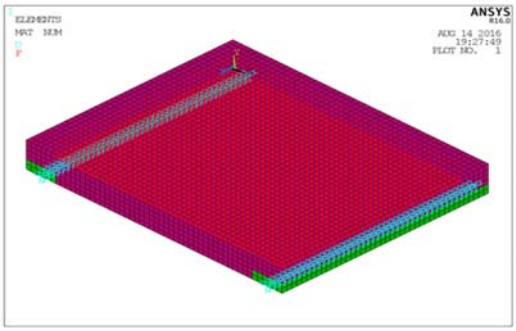

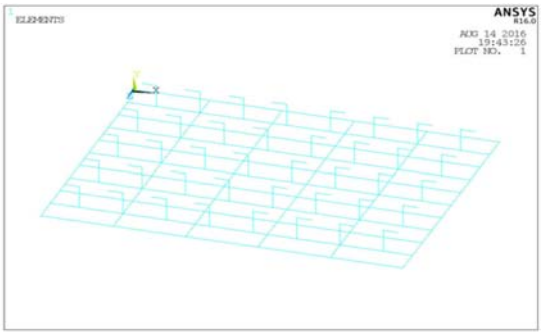

Figure 28: The model mesh and the elements dimensions Figure 29: The steel reinforcement elements (S11, S21)

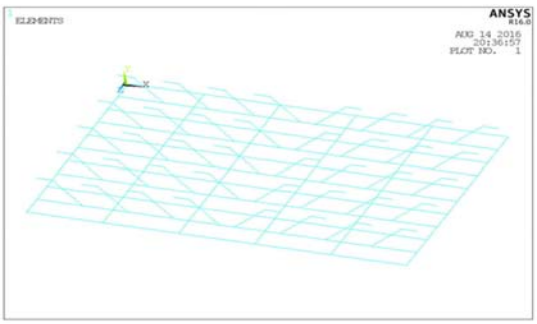

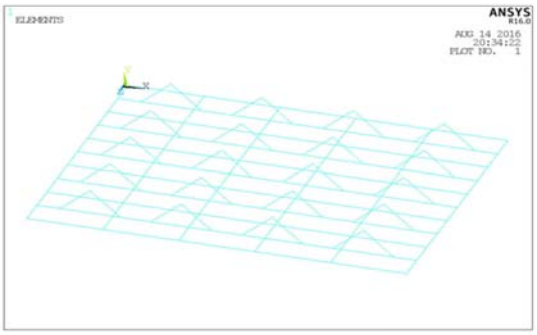

Figure 30 : The steel reinforcement elements **Figure 31: The steel reinforcement elements**

6-CONCLUSIONS

This study led the following conclusion:

1- Using of shear connector shape (2) achieved the higher result than the both shape (1) and shape (3) in each groups, with ratio 45% in G1 and G2.
2- The difference in the increasing of ultimate load result between the shapes (1), (3) and shapes (3), (2) approximately the same.
3- Changing of interface position by increasing the bottom layer led to increasing in ultimate load up to 37%.
4- Effect of interface position and concrete compressive strength appeared strongly with using of shear connector shape (1).
5- The theoretical program was able to achieve acceptable results it's up to 75% from the experimental tests in all specimens.
6- The shear resistance increases with the increase of slab thickness. When the ratio of slab thickness to beam thickness increase from 13 % to 27 % the shear failure loads increases by ratio 45 %.
7- The slab enclosed by stirrups helps to increase the shear resistance, where the shear failure loads increases by ratio ranging from 14 % to 15 %.

8- The closed stirrups help also in decreases the cracks between the slab and the web.
9- The shear failure of group G1 was more ductile than group G2.
10- The shear failure modes of light weight concrete beams are similar to normal weight concrete beams.

REFERENCES

1. W.A. Thanoon, Y. Yardim, M. S. Jaafar, and J. Noorzaei, “Development of interlocking mechanism for shear transfer in composite floor” Construction and building materials 24,2010, pp. 2604-2611.
2. Abd El-Hay A.S., “ shear transfer in composite continuous one way pre-slabs”, PHD thesis, Faculty of Engineering, Cairo University 2006.
3. Hwang S.J., Hsin-Wan Yu, and Lee H. J., “Theory of interface shear capacity of reinforced concrete”, Journal of Structural Engineering, Vol. 126, No. 12, Dec. 2000, pp. 1458-1465.
4. M. El-Sayed, ”Behavior or simply supported high strength concrete composite T-beams”, M.sc. thesis, Faculty of Engineering, Cairo University 2002.
5. P. Vainiunas, J. Valivonis, G. Marciukaitis, and B. Jonaitis, “Analysis of longitudinal shear behavior for composite steel and concrete slabs”, Journal of Constructional steel Research 62, 2006, pp. 1264-1269.